

QCD INSTANTONS AT HERA*

MICHAEL KUHLEN

*Max-Planck-Institut für Physik, Werner-Heisenberg-Institut
Föhringer Ring 6, D-80805 München, Germany*

E-mail: kühlen@desy.de

ABSTRACT

Phenomenological aspects of chirality violating processes induced by QCD instantons in deep inelastic scattering are discussed. First instanton searches and the prospects for their experimental discovery at HERA are presented.

1. Introduction

Since a long time it has been recognized that the standard model contains processes which cannot be described by perturbation theory, and which violate classical conservation laws like baryon number (B) and lepton number (L) in the case of the electroweak interaction, and chirality (Q_5) in the case of the strong interaction¹. Such anomalous processes are induced by so-called instantons². The name indicates that these are non-perturbative fluctuations that are confined to “an instant” in space-time, with no corresponding free particle solutions for $t \rightarrow \pm\infty$. The interest in instantons remained somewhat academic, as observable effects were predicted to exist only at extremely high energies of $\mathcal{O}(10^5 \text{ TeV})$, until it was discovered that their exponential suppression is much reduced by the emission of gauge bosons³. In electroweak theory with massive gauge bosons still rather high energies of $\mathcal{O}(\gtrsim 10 \text{ TeV})$ would be required, but not so in QCD with massless gluons and strong coupling. Instanton effects could play a rôle in QCD reactions already at present day colliders. Deep inelastic ep scattering at HERA is particularly interesting, because the virtuality of the photon probe Q^2 provides a hard scale for the instanton subprocess, which is needed for theoretically sound predictions^{4,5,6}. Instanton effects have not yet been observed in nature. Their experimental discovery would be of fundamental significance for particle physics.

In this report a short introduction to the basic theoretical ideas will be given. Instanton phenomenology in deep inelastic scattering (DIS) will be discussed, covering cross sections and event topologies. Finally, prospects for instanton searches and first

*invited talk at the Ringberg Workshop “New Trends in HERA Physics”, Schloß Ringberg, Tegernsee, May 1997.

results from the analysis of HERA data will be presented.

2. Instanton theory

Instantons originate from the non-trivial topological structure of the vacuum in non-Abelian gauge field theories, where the vacuum is degenerate in the Chern-Simons number N_{CS} . N_{CS} is defined as an integral over the gauge fields A_μ^a with coupling g ,

$$N_{CS} := \frac{g^2}{16\pi^2} \int d^3x \epsilon_{ijk} \left(A_i^a \partial_j A_k^a - \frac{g}{3} \epsilon_{abc} A_i^a A_j^b A_k^c \right). \quad (1)$$

Neighbouring vacua have the same (minimal) potential energy, but differ in their topological winding number N_{CS} , and are separated by a potential barrier of height E_B (fig. 1).

The usual perturbative expansion of the scattering amplitudes in the coupling constant α around *one* minimum (fig. 1), conveniently represented by a series of Feynman graphs, does not allow for transitions between neighbouring minima. They may however occur classically when the energy E is large enough $E > E_B$, or by quantum mechanical tunnelling when $E < E_B$, corresponding to so-called instanton solutions of the classical field equations. The transition amplitude for the instanton-induced tunnelling process is exponentially suppressed $\propto \exp(-4\pi/\alpha)$, a very small number.

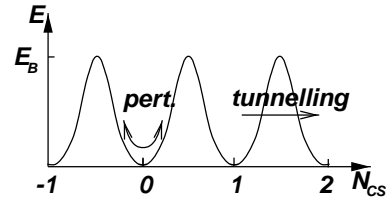


Fig. 1. The structure of the vacuum. Instanton solutions represent tunnelling transitions between topological inequivalent minima, which cannot be reached perturbatively.

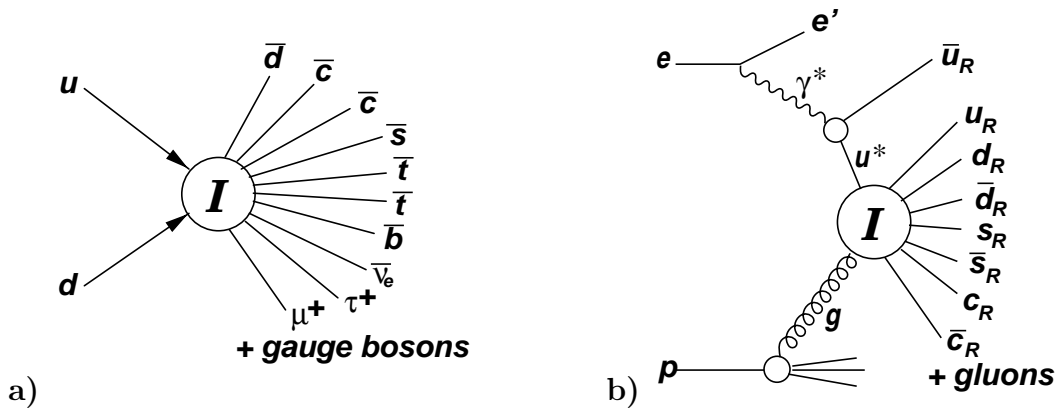


Fig. 2. a) the electroweak interaction with $\Delta(B + L) = -6$ and in b) the strong interaction with $\Delta Q_5 = 8$.

In the electroweak theory, the minimal barrier height is $E_B \approx m_W/\alpha_w = \mathcal{O}(10\text{TeV})$. Instanton transitions between vacua separated by ΔN_{CS} (see fig. 2a for an example)

would violate baryon (B) and lepton numbers ($L = L_e + L_\mu + L_\tau$) according to

$$\Delta(B + L) = -2 n_{\text{gener.}} \cdot \Delta N_{\text{CS}} , \quad (2)$$

but respect

$$\Delta(B - L) = 0 \quad \Delta L_e = \Delta L_\mu = \Delta L_\tau = \Delta B/3. \quad (3)$$

$n_{\text{gener.}} = 3$ is the number of fermion generations.

In instanton induced QCD reactions (see fig. 2b) chirality is violated. The chirality Q_5 is the difference between the number of left- and right-handed fermions, $Q_5 = \#L - \#R$. For n_f active quark flavours, the selection rule is

$$\Delta Q_5 = 2 n_f \cdot \Delta N_{\text{CS}} . \quad (4)$$

The minimal barrier height is given by the hard scale of the process, e.g. $E_B = \mathcal{O}(Q)$ for DIS⁵. The exponential suppression is less severe than in the electroweak case, because $\alpha_s \gg \alpha_w$.

3. Instantons at HERA

In recent years, it has been realized^{5,6,7,8,9,10} that quantitative calculations are possible for processes induced by QCD instantons in DIS due to the presence of a hard scale, Q^2 . In DIS, events due to QCD instantons I (and anti-instantons \bar{I}) are predominantly produced in a photon-gluon fusion processes^a (Fig. 3)

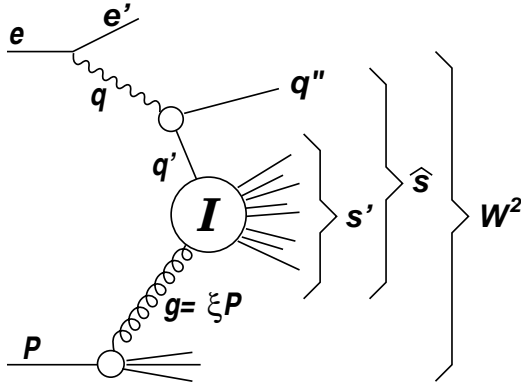
$$\gamma^* + g \xrightarrow{I} \sum_{n_f} (\bar{q}_R + q_R) + n_g g \quad \gamma^* + g \xrightarrow{\bar{I}} \sum_{n_f} (\bar{q}_L + q_L) + n_g g. \quad (5)$$

In each event, quarks and antiquarks of all n_f active flavours are found, with n_g gluons in addition.

The kinematics is depicted in fig. 3. The DIS variables Bjorken x and Q^2 can be measured from the scattered electron, $q = e - e'$. A measurement of the other variables is more challenging. A measurement of the invariant mass of the hadronic system, excluding the remnant, would determine \hat{s} . If the outgoing ‘‘current jet’’ could be identified and measured, its 4-momentum q'' would determine $q' = q - q''$, and thus the variables x' and Q'^2 which characterise the instanton subprocess. In practice, when not all of the five independent invariants (for example $x, Q^2, x', Q'^2, \hat{s}$) can be measured, they are being integrated over.

The instanton induced cross section is given by a convolution of the probability to find a gluon in the proton $P_{g/p}$, the probability that the virtual photon splits

^aQuark initiated processes have not yet been considered. Due to the large gluon content of the proton in the HERA domain at small x , they are expected to be of minor importance. In addition, they are expected to be suppressed by $\mathcal{O}(\alpha_s^2)$ with respect to the gluon initiated processes.



DIS variables:

$$\begin{aligned}
 Q^2 &:= -q^2 \\
 x &:= Q^2 / (2P \cdot q) \\
 W^2 &:= (q + P)^2 = Q^2 (1 - x)/x \\
 \hat{s} &:= (q + g)^2 \\
 \xi &= x(1 + \hat{s}/Q^2)
 \end{aligned}$$

Variables of instanton subprocess:

$$\begin{aligned}
 Q'^2 &:= -q'^2 \\
 x' &:= Q'^2 / (2g \cdot q') \\
 s' &:= (q' + g)^2 = Q'^2 (1 - x')/x'
 \end{aligned}$$

Fig. 3. Kinematics of instanton induced processes in DIS. The labels denote the 4-vectors of the particles. A virtual photon γ^* (4-momentum $q = e - e'$) emitted from the incoming electron fuses with a gluon (4-momentum g) from the proton (4-momentum P). The gluon carries a fraction ξ of the proton momentum. The virtual quark q^* entering the instanton subprocess has 4-momentum q' , and the outgoing quark from the $\gamma^* \rightarrow q\bar{q}$ splitting has 4-momentum q'' . The invariant masses squared of the γ^*g and q^*g systems are \hat{s} and s' . W is the invariant mass squared of the total hadronic system (the γ^*p system). $0 \leq x \leq x/\xi \leq x' \leq 1$ holds. For completeness, we note $y := (Pq)/(Pe) = Q^2/(sx)$, where $s = (e + P)^2$ is the ep invariant mass squared.

into a quark-antiquark pair in the instanton background $P_{q^*/\gamma^*}^{(I)}$, and the cross section $\sigma_{q^*g}^{(I)}(x', Q'^2)$ of the instanton subprocess^{6,7}. Multi-gluon emission enhances the cross section³

$$\sigma_{q^*g;n_g}^{(I)} \propto \frac{1}{n_g!} \left(\frac{1}{\alpha_s}\right)^{n_g} \exp(-4\pi/\alpha_s). \quad (6)$$

The cross section of the instanton induced subprocess is then⁶:

$$\sigma_{q^*g}^{(I)}(x', Q'^2) = \sum_{n_g=0}^{\infty} \sigma_{q^*g;n_g}^{(I)} \approx \frac{\Sigma(x')}{Q'^2} \left(\frac{4\pi}{\alpha_s(\mu(Q'))}\right)^{\frac{21}{2}} \exp\left(\frac{-4\pi}{\alpha_s(\mu(Q'))} F(x')\right). \quad (7)$$

It depends critically on the functions $F(x')$ (called the “holy grail” function), which modifies the exponent in the suppression factor $\exp(-4\pi/\alpha_s)$, and on $\Sigma(x')$, which depends on $F(x')$. There exists also a scale dependence due to the choice of the renormalization scale $\mu(Q')$.

$F(x')$ can be estimated reasonably well (see fig. 4) for x' not too small, $x' \gtrsim 0.2$ ⁶. The extrapolation to lower values of x' is unreliable due to inherent ambiguities. In addition, multi-

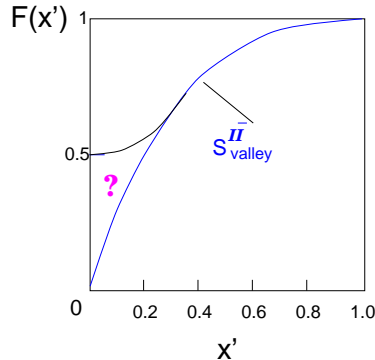


Fig. 4. The holy grail function $F(x')$ ⁶. For small s' ($x' \approx 1$), instanton perturbation theory is applied. The calculation with the valley method matches smoothly with the perturbative result.

instanton effects should be avoided by limiting the instanton size ρ_I (the spatial region occupied during the interaction) to $\rho_I < 2 \text{ GeV}^{-1}$ with a cut-off $Q'^2 \gtrsim 25 \text{ GeV}^2$ ^{6,7}. That requirement ensures also that $\alpha_s(\mu(Q'))$ stays small enough to apply instanton perturbation theory.

The resulting instanton induced subprocess cross section $\sigma_{q^*g}^{(I)}(x', Q'^2)$ (see fig. 5) is peaked at $Q' \approx 5 \text{ GeV}$ and exponentially grows with decreasing x' . The integrated instanton induced ep DIS cross section (see fig. 6) is sizeable; for $x > 0.001$ and $x' > 0.2$ it is of $\mathcal{O}(10 \text{ pb})$. The cross section is approximately scaling (depends only on x , not on Q^2 for large Q^2) ⁷. It grows towards small x , and increases dramatically when the lower x' cut-off is relaxed. Eventually higher order instanton effects have to dampen the growth of the cross section.

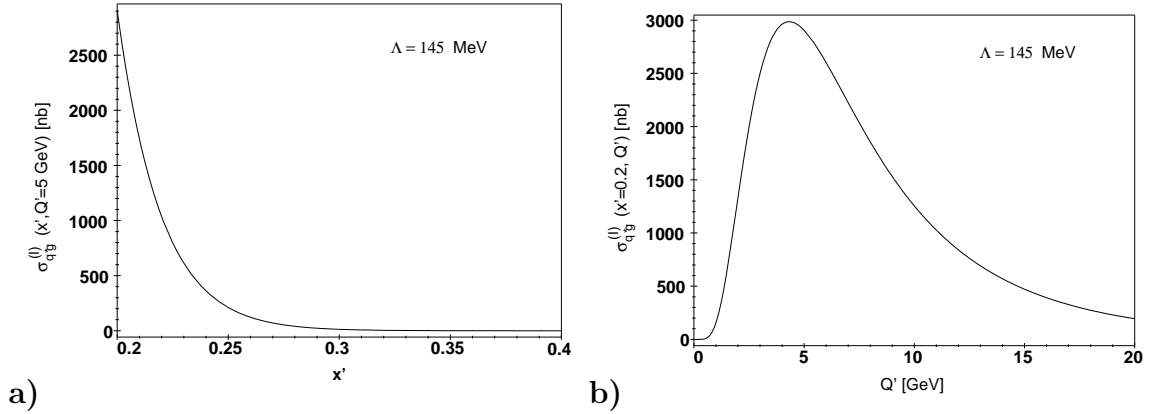


Fig. 5. The instanton subprocess cross section⁹ for $q^*g \rightarrow \text{hadrons}$ as a function of **a)** x' for $Q' = 5 \text{ GeV}$ and **b)** Q' for $x' = 0.2$.

Two kinematic regions have to be distinguished. For $x' > 0.2$ the predictions are relatively safe, allowing the instanton theory to be tested. Either instantons are discovered at the predicted level – including the substantial theoretical uncertainties, which still need to be quantified –, or the theory has to be revised. For $x' < 0.2$ the cross section presumably continues to grow, but the extrapolation is extremely uncertain. For a discovery, this is the favourable region due to the large cross section. A negative result however cannot be turned against the theory, it would rather restrict the unknown behaviour of $F(x')$ at small x' . Most promising is the kinematic region of small Bjorken- x , because both the total DIS cross section and the predicted fraction of instanton induced events increase towards small x (see fig. 9b).

4. Experimental signatures

In the theoretically safe region, $x' > 0.2$, the expected fraction of instanton events in all DIS events is of $\mathcal{O}(10^{-3} - 10^{-4})$ (compare fig.9b), too small to be detected in inclusive cross section measurements (i.e. the structure function F_2). Instead,

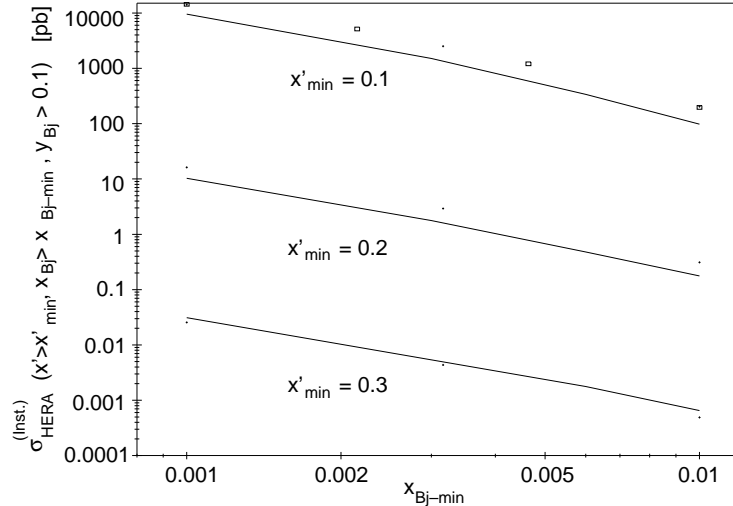


Fig. 6. The instanton induced DIS cross section⁹ $ep \rightarrow e'X$ integrated over Bjorken $x > x_{\text{min}}$, $y > 0.1$, and over the regions $Q' > 5$ GeV and $x' > x'_{\text{min}}$ as indicated.

dedicated searches for the characteristic features of instanton events in the hadronic final state have to be performed. A Monte Carlo generator (QCDINS¹¹) to simulate the hadronic final state of instanton events in DIS is available. In general, the event shape predictions are more stable than the rate predictions, because poorly known factors cancel. The instanton event properties can be contrasted with predictions from event generators for normal DIS events (ARIADNE¹², LEPTO¹³ and HERWIG¹⁴) which give an overall satisfactory description of the DIS final state properties¹⁵.

In the q^*g rest frame $2n_f - 1$ quark and antiquarks and n_g gluons are emitted isotropically from the instanton subprocess. n_g is Poisson distributed with^{7,9}

$$\langle n_g \rangle \approx \frac{2\pi}{\alpha_s} x'(1-x') \frac{dF(x')}{dx'}. \quad (8)$$

After hadronization, this leads to a spherical system with a high multiplicity of hadrons, depending mainly on the available centre of mass energy $\sqrt{s'} = Q' \sqrt{1/x' - 1}$. For a typical situation ($x' = 0.2$, $Q' = 5$ GeV $\Rightarrow \sqrt{s'} = 10$ GeV), $\langle n_g \rangle = \mathcal{O}(2)$. About $n_p = 10$ partons and $n = 20$ hadrons are expected. The expected parton momentum spectrum is semi-hard⁵ with transverse momentum $\langle p_T \rangle \approx (\pi/4)(\sqrt{s'}/\langle n_p \rangle)$.

Hadronic final state properties are conveniently being studied in the centre of mass system (CMS) of the incoming proton and the virtual boson, i.e. the CMS of the hadronic final state. Longitudinal and transverse quantities are calculated with respect to the virtual boson direction (defining the $+z$ direction). The pseudorapidity η is defined as $\eta = -\ln \tan(\theta/2)$, where θ is the angle with respect to the virtual photon direction. When boosted to the CMS, the hadrons emerging from the instanton subprocess occupy a band in pseudorapidity of half width $\Delta\eta \approx 1$, which is homogeneously populated in azimuth⁵.

The characteristics of instanton events by which they can be distinguished from normal DIS events are therefore: high multiplicity with large transverse energy; spherical event configuration (apart from the current jet); and the presence of all flavours (twice!) that are kinematically allowed in each event. One would therefore look for events which in addition to the other characteristics are rich in K^0 s, charm decays, secondary vertices, muons etc.. In general, the strength of instanton signals in the hadronic final state increases somewhat towards low x' and large Q'^2 due to the increasing “instanton mass” $\sqrt{s'} = Q' \sqrt{1/x' - 1}$.

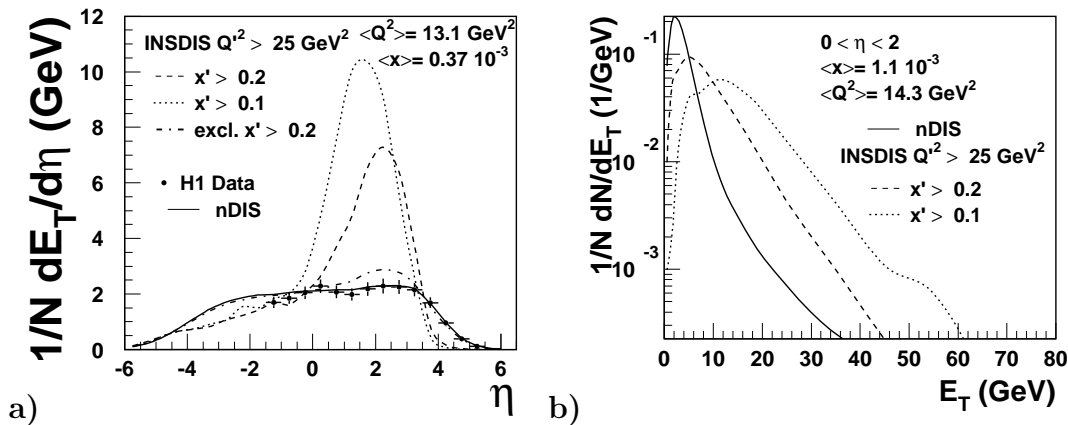


Fig. 7. Transverse energy E_T in the hadronic CMS ¹⁶. **a)** The E_T flow vs. η . The proton remnant direction is to the left. The standard QCD model (nDIS=ARIADNE) and different instanton scenarios are confronted with the H1 data ¹⁷. The excluded scenario ¹⁶ with an instanton fraction $f_I > 11.8\%$ for $x' > 0.2$ is indicated. **b)** The E_T distribution, where the transverse energy is measured in the CMS rapidity bin $0 < \eta < 2$, for two instanton scenarios, and the standard QCD model (nDIS=ARIADNE). The plots are normalized to the total number of events N that enter the distributions.

The “instanton band” shows up in the flow of hadronic transverse energy E_T as a function of η (fig. 7a). It’s height and position depends on x' and Q'^2 (and also on x and Q^2). In normal DIS events on average an E_T of 2 GeV per η unit is observed. In instanton induced events, that number may go up to 10 GeV for low x' . A possible search strategy could involve the E_T distribution in a selected rapidity band (fig. 7b), looking for high E_T events in the tail of the distribution^{18,16}.

Further discrimination can be obtained¹⁸ from the fact that for instanton events the E_T should be distributed isotropically, while normal DIS events are jet-like, in particular for large E_T . One defines

$$E_{\text{out}} := \min \sum_i \vec{p}_i \cdot \vec{n} \qquad E_{\text{in}} := \sum_i \vec{p}_i \cdot \vec{n}' \qquad (9)$$

The sum runs over all final state hadrons i with momentum \vec{p}_i . \vec{n} is the unit vector perpendicular to the virtual photon axis which minimizes E_{out} and thus defines the event plane. \vec{n}' lies in the event plane and is normal to both \vec{n} and the virtual photon

axis. It is easy to show that for an ideal isotropic “instanton decay”, $E_{\text{out}} = \sqrt{s'}/2$ ¹⁸. The “instanton mass” $\sqrt{s'}$ can thus be reconstructed experimentally (fig. 8a). Normal DIS events, either “1+1” or “2+1” jet events (the +1 refers to the unobserved proton remnant) are contained in the event plane, $E_{\text{out}} \ll E_{\text{in}}$, in contrast to instanton events with $E_{\text{out}} \approx E_{\text{in}}$ (see fig. 8b).

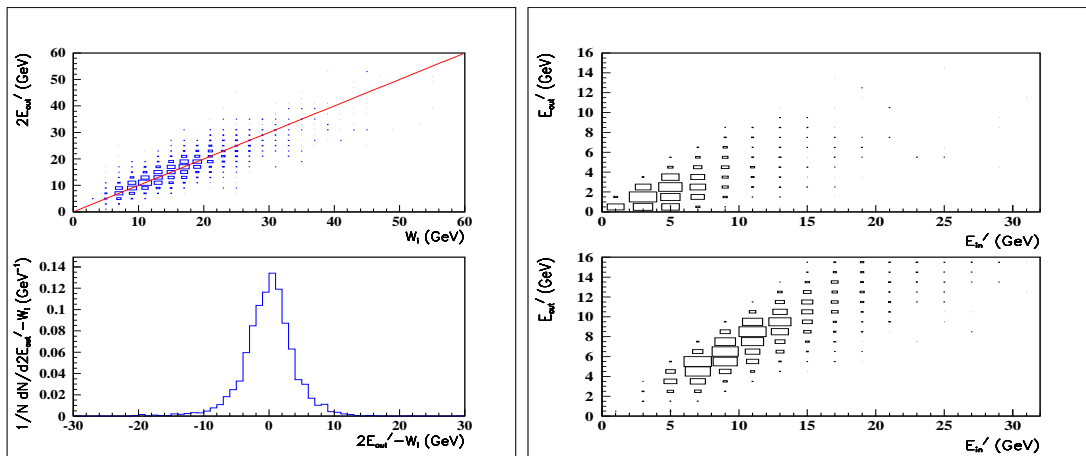


Fig. 8. **a)** The correlation between $2 \cdot E'_{\text{out}}$ and the “instanton mass”, $W_I = \sqrt{s'}$ (top), and the resolution for $\sqrt{s'}$ that can be achieved (bottom)¹⁸. The primes indicate additional cuts in η to minimize higher order QCD radiation which may wash out the relation between E_{out} and $\sqrt{s'}$. **b)** E'_{out} vs. E'_{in} for normal (top, HERWIG) and instanton induced events (bottom, QCDINS)¹⁸. Both distributions are taken in the hadronic CMS for events with $0.001 < x < 0.01$, $0.1 < y < 0.6$ and $20 \text{ GeV}^2 < Q^2 < 70 \text{ GeV}^2$.

Instanton events are characterized by a large particle density localized in rapidity. In normal DIS events there are about 2 charged particles per unit of pseudorapidity¹⁹, rather uniformly distributed in η . For a low x' cut-off, that number goes up to 10 in the peak of the instanton band¹⁶. Very sensitive to instanton events is the charged particle multiplicity distribution¹⁶, see fig. 9a. A significant fraction of the instanton events would lead to charged multiplicities which are very unlikely to be found in normal DIS events. Furthermore, particle-particle correlation functions should be influenced by instanton effects²⁰.

5. Searches for instanton processes

The fact that instanton events look very different from the expectation for standard QCD events can be exploited to search for instanton signals in the HERA data. One strategy is to compare the shape of hadronic final state distributions to the expectation from standard QCD events (nDIS) with an admixture of instanton events (INSDIS) of fraction f_I . In case the measured distribution agrees with the standard QCD expectation, a limit on the fraction of instanton induced events in DIS $f_I < f_{\text{lim}}$ can be set. The caveat of this method is that one has to make an assump-

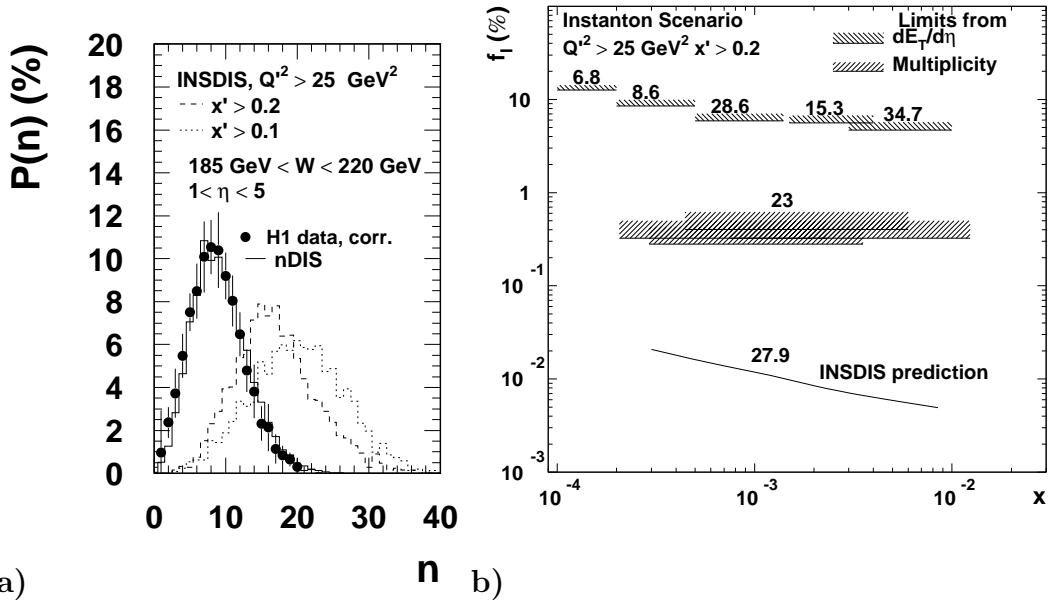


Fig. 9. **a)** The probability distribution $P(n)$ of the charged particle multiplicity n from the CMS pseudorapidity range $1 < \eta < 5$ for events with $185 \text{ GeV} < W < 220 \text{ GeV}$. Shown are the unfolded H1 data ²¹, the expectation from a standard DIS model (nDIS=ARIADNE)), and the predictions for instanton events with different cut-off scenarios ¹⁶. **b)** The maximally allowed fraction f_{lim} of instanton induced events in DIS for $Q'^2 > 25 \text{ GeV}^2$ and $x' > 0.2$ from transverse energy flows and the multiplicity distribution as function of x ¹⁶. Regions above the lines are excluded at 95% C.L.. The numbers give the average Q^2 values in GeV^2 for the x bins. The theory prediction, calculated with QCDINS ¹¹, for $10 \text{ GeV}^2 < Q^2 < 80 \text{ GeV}^2$ is superimposed (full line, label INSDIS).

tion on what standard QCD looks like. In particular at small x that issue is under debate ^{22,23,24}. There exists a danger that an instanton effect is tuned or explained away by stretching the standard QCD predictions by generator tuning, introducing for example BFKL effects etc.. A good understanding of standard QCD will be crucial for the positive identification of instanton effects.

In the first search for instanton events²⁵ an anomalous K^0 yield has been looked for. For $x > 10^{-3}$ about 0.12 K^0 mesons (including \bar{K}^0) have been measured per event and unit pseudorapidity, with a relatively flat η distribution. For instanton events with $x' > 0.2$, a peaked distribution with about 0.55 K^0 per event and unit η is expected. From the comparison with standard QCD event generators^{12,13,14} and the instanton generator¹¹ an upper limit of $f_I < f_{\text{lim}} = 6\%$ at 95% C.L. is obtained²⁵.

The charged particle multiplicity distribution $P(n)$ in high energy reactions can often be described by a negative binominal distribution (NBD). Also the DIS data are relatively well described by NBDs ²¹. The multiplicity distribution from the CMS interval $1 < \eta < 5$ for events with $W = 80 - 115 \text{ GeV}$ (corresponding to $x > 0.0007$) can be parametrized with an NBD of mean $\langle n \rangle = 6.90 \pm 0.33$. Possible deviations from an NBD allow for an instanton fraction of at most $f_I = 2.7\%$ at 95% C.L. ²¹.

Other measured event shapes have been systematically analysed in terms of their

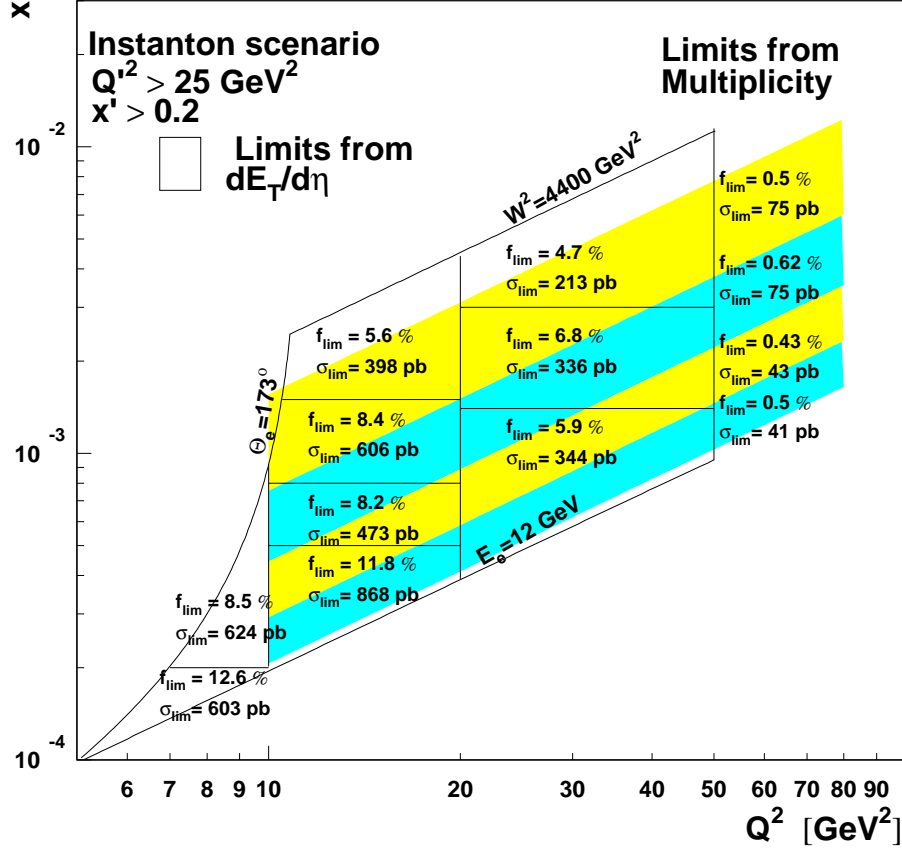


Fig. 10. 95% C.L. limits on instanton production with $Q'^2 > 25 \text{ GeV}^2$ and $x' > 0.2$ ¹⁶. The cross-section limits (σ_{lim}) together with the maximally allowed instanton fraction f_{lim} are shown in the $x - Q^2$ plane. They are obtained from the E_T flow analysis (open fields), and from the multiplicity analysis (shaded fields) with their numbers at the right edge. The boundaries implied by the analysis cuts of the energy flow analysis in the angle and energy of the scattered electron, $\theta_e < 173^\circ$ and $E_e > 12 \text{ GeV}$, and by the requirement $W^2 > 4400 \text{ GeV}^2$ are indicated.

sensitivity to instanton events¹⁶, and their dependence on the kinematic variables x, Q^2, x', Q'^2 . The most sensitive distributions were the transverse energy flows¹⁷, the pseudorapidity distribution of charged particles and their p_T spectra¹⁹. For example, the E_T flow has been measured over a wide range of x and Q^2 , allowing to extend the search region down to $x = 0.0001$. From a shape analysis¹⁶ (see fig. 7), instanton fractions f_I between 5 and 13 % can be excluded for $x' > 0.2$ (see figs. 9b, 10). For lower x' the signal is more prominent, and somewhat better limits are obtained.

The fact that H1²¹ did not observe any events above a certain multiplicity n_{max} has been exploited¹⁶ to place more stringent limits on instanton production^b. A significant fraction of instanton induced events would have multiplicities $n > n_{\text{max}}$

^bThe previous limits from the H1 multiplicity analysis²¹ were derived from the shape of the multiplicity distribution for $n < n_{\text{max}}$.

Table 1. Limits on QCD instantons in DIS. A fraction $f_I > f_{\text{lim}}$ of instanton induced events in DIS is excluded at 95% C.L..

analysis	DIS kinematics covered			instanton scenario		limit
	Q^2 (GeV ²)	x	W (GeV)	Q^2 (GeV ²)	x'	f_{lim}
K^0 ²⁵	10 – 70	0.001 – 0.01	95 – 230	$\gtrsim 1$	$\gtrsim 0.2$	6 %
multipl. ²¹	10 – 80	0.0007 – 0.012	80 – 115	$\gtrsim 1$	$\gtrsim 0.2$	2.7 %
E_T flows ¹⁶	5 – 50	0.0001 – 0.01	65 – 230	> 25	> 0.2	5 – 13 %
multipl. ¹⁶	10 – 80	0.0001 – 0.01	80 – 220	> 25	> 0.2	0.4 – 0.6 %

(compare fig. 9a). Instanton fractions $f_I > 0.4 - 0.6\%$ can therefore be excluded for $x' > 0.2$ (see figs. 9b, 10), and somewhat lower f_I values for a lower cut-off $x' > 0.1$ ¹⁶. This search method has the advantage that, in contrast to the previous shape comparisons, it does not rely on assumptions for standard QCD event topologies, since no background needs to be subtracted. Unavoidable of course is the dependence on the expected instanton event shape, which may be even more uncertain than the standard QCD event shapes.

The available bounds on instanton production are summarised in tab. 1. The most stringent limits for the theoretically “safe” scenario $x' > 0.2$ are still a factor 20 higher than what is predicted from the instanton theory, see fig. 9b. Limits for other scenarios can be found in ¹⁶. For $x' > 0.1$ they are already below the naive extrapolation into the theoretically uncertain region, providing a constraint for the theory and the holy grail function $F(x')$.

6. Conclusion

Instanton transitions, a yet unexplored facette of non-abelian gauge field theories, have been discussed. While in the electroweak theory the $B + L$ violating effects induced by instantons are expected only at energies $\gtrsim 10$ TeV, their chirality violating pendant in QCD could lead to striking signatures already at present day colliders. In DIS at HERA, these are a high particle multiplicity with large transverse energy localized in rapidity, and s , c and possibly b quarks in the final state. The expected contribution to DIS events is of $\mathcal{O}(10^{-3} - 10^{-4})$, with substantial theoretical uncertainties. First analysis of HERA data taken in the years ≤ 1994 , corresponding to an integrated luminosity of $\mathcal{O}(1.3 \text{ pb}^{-1})$, are still a factor ≈ 20 above the prediction. With higher statistics data samples ($\mathcal{O}(25 \text{ pb}^{-1})$ up to summer 1997) and improved search strategies, a fundamental discovery at HERA appears to be in reach. It might be possible to exploit also other reactions than DIS, such as photoproduction, where the hard scale needed for reliable instanton calculations could be provided by the p_T of a jet.

7. Acknowledgements

I would like to thank B. Kniehl and G. Kramer for their invitation to this beautifully set workshop, and I thank T. Carli, A. Ringwald and F. Schrempp for the exciting time we are having with instantons, and for their critical reading of the manuscript.

8. References

1. G. 't Hooft, Phys. Rev. Lett. 37 (1976) 8; Phys. Rev. D14 (1976) 3432.
2. A. Belavin, A. Polyakov, A. Schwarz and Yu. Tyupkin, Phys. Lett. B59 (1975) 85.
3. A. Ringwald, Nucl. Phys. B330 (1990) 1; O. Espinosa, Nucl. Phys. B343 (1990) 310.
4. I.I. Balitskii and V.M. Braun, Phys. Lett. B314 (1993) 237.
5. A. Ringwald and F. Schrempp, DESY 94-197, hep-ph/9411217, Proc. of Int. Sem. "Quarks 94", Vladimir, Russia, 1994, p. 170.
6. A. Ringwald and F. Schrempp, DESY 96-203, hep-ph/9610213, to appear in Proc. IXth Int. Sem. "Quarks 96", Yaroslavl, Russia, 1996.
7. S. Moch, A. Ringwald and F. Schrempp, DESY 96-202 hep-ph/9609445; and in prep.
8. A. Ringwald and F. Schrempp, DESY 96-125, hep-ph/9607238, Proc. of the Workshop DIS 96 on "Deep Inelastic Scattering and Related Phenomena", Rome 1996, eds. G. D'Agostini and A. Nigro, p. 481.
9. A. Ringwald and F. Schrempp, DESY 97-115, hep-ph/9706399, to appear in Proc. of the DIS97 workshop, Chicago 1997, eds. J. Repond and D. Krakauer.
10. S. Moch, A. Ringwald and F. Schrempp, DESY 97-114, hep-ph/9706400, to appear in the Proc. of the DIS97 workshop, Chicago 1997, eds. J. Repond and D. Krakauer.
11. T. Carli, M. Gibbs, M. Kuhlen, A. Ringwald and F. Schrempp, in preparation (version used: QCDINS 1.4.1).
12. L. Lönnblad, Comp. Phys. Comm. 71 (1992) 15 (version used: 4.08).
13. G. Ingelman, Proc. of the Workshop on Physics at HERA, Hamburg 1991, eds. W. Buchmüller and G. Ingelman, vol. 3, p. 1366; G. Ingelman, A. Edin and J. Rathsman, DESY 96-057.
14. G. Marchesini et al., Comp. Phys. Comm. 67 (1992) 465 .
15. N. Brook et al., Proc. of the Workshop on Future Physics at HERA, Hamburg 1996, eds. G. Ingelman, A. DeRoeck and R. Klanner, vol. 2, p. 613.
16. T. Carli and M. Kuhlen, DESY 97-151, MPI-PhE/97-18, hep-ex/9708008, to appear in Nucl. Phys. B.
17. H1 Collab., S. Aid et al., Phys. Lett. B356 (1995) 118.
18. M. Gibbs, T. Greenshaw, D. Milstead, A. Ringwald and F. Schrempp, Proc. of the Workshop on "Future Physics at HERA", Hamburg 1996, eds. G. Ingelman, A. DeRoeck and R. Klanner, vol. 1, p. 509.
19. H1 Collab., C. Adloff et al., Nucl. Phys. B485 (1997) 3.
20. V. Kuvshinov and R. Shulyakovsky, Acta Physica Polonica B28 (1997) 1629.
21. H1 Collab., S. Aid et al., Z. Phys. C72 (1996) 573.
22. T. Carli, to appear in Proc. of the Ringberg Workshop "New Trends in HERA Physics", 1997.
23. G. Grindhammer, to appear in Proc. of the Ringberg Workshop "New Trends in HERA Physics", 1997.
24. M. Kuhlen, to appear in the Proc. of the Madrid Workshop on low x Physics, 1997.
25. H1 Collab., S. Aid et al., Nucl. Phys. B480 (1996) 3.